MATERIALS SCIENCE

One-step vapor-phase synthesis of transparent high refractive index sulfur-containing polymers

Do Heung Kim[1]*, Wontae Jang[1]*, Keonwoo Choi[1], Ji Sung Choi[2], Jeffrey Pyun[3,4], Jeewoo Lim[2†], Kookheon Char[4†], Sung Gap Im[1†]

High refractive index polymers (HRIPs) have recently emerged as an important class of materials for use in a variety of optoelectronic devices including image sensors, lithography, and light-emitting diodes. However, achieving polymers having refractive index exceeding 1.8 while maintaining full transparency in the visible range still remains formidably challenging. Here, we present a unique one-step vapor-phase process, termed sulfur chemical vapor deposition, to generate highly stable, ultrahigh refractive index (n > 1.9) polymers directly from elemental sulfur. The deposition process involved vapor-phase radical polymerization between elemental sulfur and vinyl monomers to provide polymer films with controlled thickness and sulfur content, along with the refractive index as high as 1.91. Notably, the HRIP thin film showed unprecedented optical transparency throughout the visible range, attributed to the absence of long polysulfide segments within the polymer, which will serve as a key component in a wide range of optical devices.

INTRODUCTION

High refractive index polymers (HRIPs) (*1*), which generally refer to polymers having refractive index (n) of greater than 1.6, are a class of materials studied extensively because of their key role in a wide range of optoelectronic applications (*1*–*3*). Because inorganic semiconductors in advanced optical devices usually have n > 1.8, HRIPs with similar refractive index are of substantial interest for practical applications since polymers exhibit (i) superior mechanical flexibility, (ii) better capability of fine-tuning of properties through chemical modification, (iii) processability into a wide range of forms including molded lenses, thin films, coatings, and composites, (iv) lighter weight, and (v) lower cost compared to their inorganic counterparts. To date, however, n of 1.8 in the visible and near–infrared (IR) region is generally regarded as an upper limit in noncomposite polymers. A widely used design principle for HRIPs involves the incorporation of functional groups with high molar refraction into the HRIPs, where the most widely used ones often contain sulfur (*4*, *5*). Since the refractive index of polymers increases with increasing content of high molar refraction functional groups, direct polymerization of elemental sulfur, such as inverse vulcanization, to achieve high-sulfur content polymers was suggested as an attractive strategy toward HRIPs (*1*, *2*, *6*–*8*). However, elemental sulfur is generally not quite miscible with most organic compounds (*9*), which strongly limits their application to generate a wide range of sulfur-containing polymers (SCPs). Moreover, formation of long polysulfide chains is inevitable in the polymers synthesized from elemental sulfur, which are highly susceptible to depolymerization to monomeric cyclooctasulfur (S_8) (*9*–*11*). These issues must be addressed to establish reliable synthesis of sulfur-derived HRIPs with tunable properties. Another problem associated with the direct polymerization of elemental sulfur is the rapid vitrification of reaction mixture during the radical copolymerization of molten sulfur (*8*), a phenomenon that makes it extremely difficult to process the product polymers into desired forms. The unique advantage of HRIPs over other high-n materials lies in facile processing to create bespoke components, such as molded lenses, coatings, and stacks. Most of all, although n > 1.8 across the IR spectrum can be achieved from the one-step, bulk inverse vulcanization reaction (*12*, *13*), the materials show strong absorption in the lower wavelength region of the visible range, rendering them brownish red in color and thus not suitable for optical applications that require high transparency in visible range. Developing methods using elemental sulfur directly toward HRIPs with full transparency over the entire visible spectrum and n > 1.8 still remains unsolved.

We demonstrate here a previously unknown vapor-phase deposition method for sulfur polymerization, namely, sulfur chemical vapor deposition (sCVD), which allows for a one-step preparation of high sulfur content HRIPs. The process involves thermal homolytic ring opening of gaseous elemental sulfur and subsequent polymerization of the resulting radicals with vinyl-containing comonomers. A large entropic gain, a characteristic feature in gas-phase mixing, allowed for the use of various kinds of comonomers regardless of the miscibility with the elemental sulfur in the liquid phase (*14*, *15*). The vapor-phase method was used to generate highly cross-linked SCP thin films directly on a wide range of substrates. One of the most remarkable findings was that the polymers from sCVD showed unprecedentedly high refractive index exceeding 1.9 while being fully transparent in the entire visible range, which is in marked contrast to previously reported polymers from SCPs with similar sulfur contents (*1*, *6*–*7*). The SCP films also exhibited excellent environmental stability and chemical resistance, which is highly desirable for their application to long-term optical device applications.

RESULTS

Deposition apparatus and vapor deposition copolymerization of elemental sulfur

The schematic diagram of the sCVD apparatus, along with the synthetic steps of SCPs through sCVD, is illustrated in Fig. 1 (A and B),

[1]Department of Chemical and Biomolecular Engineering and KI for NanoCentury, Korea Advanced Institute of Science and Technology (KAIST) 291 Daehak-ro, Yuseong-gu, Daejeon 34141, Republic of Korea. [2]Department of Chemistry and Research Institute for Basic Science, Kyung Hee University, 26 Kyungheedae-ro, Dongdaemun-gu, Seoul 02447, Republic of Korea. [3]Department of Chemistry and Biochemistry, University of Arizona, 1306 East University Boulevard, Tucson, AZ 85721, USA. [4]The National Creative Research Initiative Center for Intelligent Hybrids, The WCU Program of Chemical Convergence for Energy and Environment, Department of Chemical and Biological Engineering, Seoul National University, Seoul 08826, Republic of Korea.
*These authors contributed equally to this work.
†Corresponding author. Email: sgim@kaist.ac.kr (S.G.I.); khchar@plaza.snu.ac.kr (K.C.); jeewoo@khu.ac.kr (J.L.)

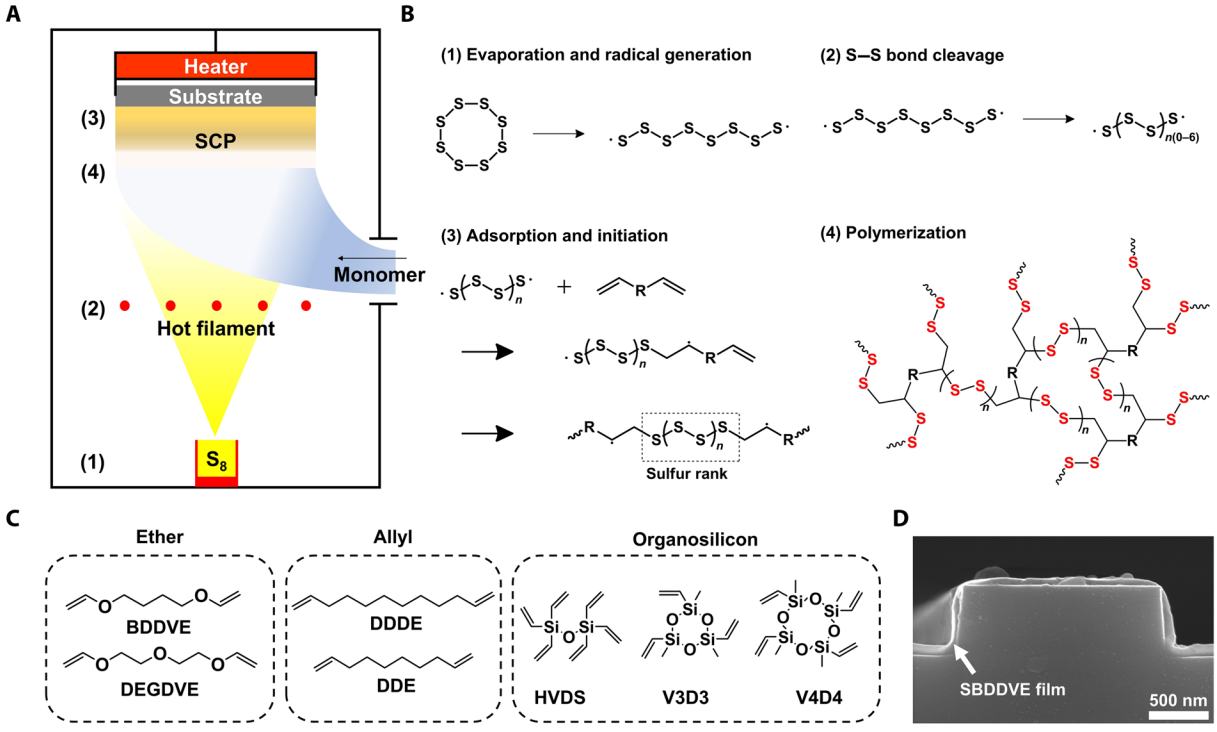

Fig. 1. Synthesis of SCP films in vapor phase. (**A**) A schematic illustration of overall sCVD system. (**B**) SCP synthesis scheme from elemental sulfur and cross-linkable comonomer: (1) elemental sulfur is evaporated from the heated crucible located at the bottom of the sCVD chamber and decomposed to form radicals; (2) the evaporated elemental sulfur is cleaved to shorter linear sulfur diradicals by hot filament; (3) the sulfur diradicals activate the vaporized monomers to propagate the free radical polymerization reaction; and (4) the heavily cross-linked SCP film is deposited on the surface of the substrate. (**C**) Cross-linkable monomers used in this study for sCVD polymerization: BDDVE, DEGDVE, DDDE (1,11-dodecadiene), DDE (1,9-decadiene), HVDS (hexavinyldisiloxane), V3D3 (1,3,5-trivinyl-1,3,5-trimethylcyclotrisiloxane), and V4D4 (1,3,5,7-tetravinyl-1,3,5,7-tetramethylcyclotetrasiloxane). (**D**) A scanning electron microscope image of the 1600-nm nanopatterned Si wafer coated conformally with 60-nm-thick SBDDVE film.

respectively. The sCVD chamber consists of a load cell for the evaporation of elemental sulfur and vapor-phase delivery system for vinyl comonomer. The substrate, equipped with a temperature-controlling unit, is located at the top of the chamber, facing down toward the sulfur load cell. The substrate temperature, T_s, not only must be low enough to allow for the adsorption of monomers and/or early polymer products but also must be high enough to propagate the polymerization reaction stably on the substrate surface. The T_s in the range of 110° to 135°C was found to be optimal for this study. The distance between the substrate and the load cell was determined so as to prevent direct heat transfer from load cell crucible while ensuring sufficient mass transfer of the reactants. An array of heating filament, located between the substrate and sulfur evaporator source, was heated to a temperature to ensure continuous generation of radicals from thermal homolytic ring opening of the evaporated sulfur in the chamber. The position and the temperature (350°C) of the heating filament array were carefully tuned. Evaporating the elemental sulfur in the sCVD chamber saturated with various comonomers vaporized from the separate load cell allowed for the deposition of polymeric thin films with high sulfur content onto the substrate. Various types of vinyl ethers, allyl compounds, and vinyl silanes including 1,4-butanediol divinyl ether (BDDVE) and di(ethylene glycol) divinyl ether (DEGDVE), which could not be copolymerized with the molten sulfur due to their lack of miscibility, could be polymerized successfully directly with the elemental sulfur through the one-step procedure (Fig. 1C), which is attributable to the homogeneous mixing of sulfur and the comonomer in the vapor phase (*16*). The vapor-phase polymerization method allowed for conformal coating of SCP thin films on various substrates, including 1600-nm nanopatterned Si wafer (Fig. 1D), glass, silicon wafer, polyethylene terephthalate (PET), polyethylene naphthalate (PEN), polydimethyl siloxane (PDMS), polyimide (PI), latex, and porous stainless steel mesh (see figs. S1 and S2). Considering the difficulty in processing high sulfur content SCP into a uniform thin film, the sCVD represents a major progress toward expanding the applicability of the SCPs to films.

Polymer characterization

Differential scanning calorimetry (DSC) conducted on the SCP polymerized from BDDVE monomer and elemental sulfur [poly(sulfur-co-1,4-butanediol divinyl ether) (SBDDVE)] showed no apparent peak associated with the transition between α and β allotropes nor the melting of elemental sulfur. Glass transition temperature (T_g) was detected from SBDDVE at 67°C and 36.5°C with 60 and 70 weight % (wt %) sulfur contents, respectively (Fig. 2A). The T_g values are higher than inverse vulcanization products between sulfur and divinylbenzene (SDVB; T_g = 31°C for 70 wt % sulfur) (*17*), which is remarkable given that SDVB contains aromatic groups, while SBDDVE from sCVD does not. The results suggest that SBDDVE from sCVD is highly cross-linked, which is consistent with x-ray photoelectron spectroscopy (XPS) data discussed below. Similarly, in thermogravimetric analysis (TGA), elemental sulfur showed total mass loss due to the complete evaporation of the elemental sulfur, while a considerable

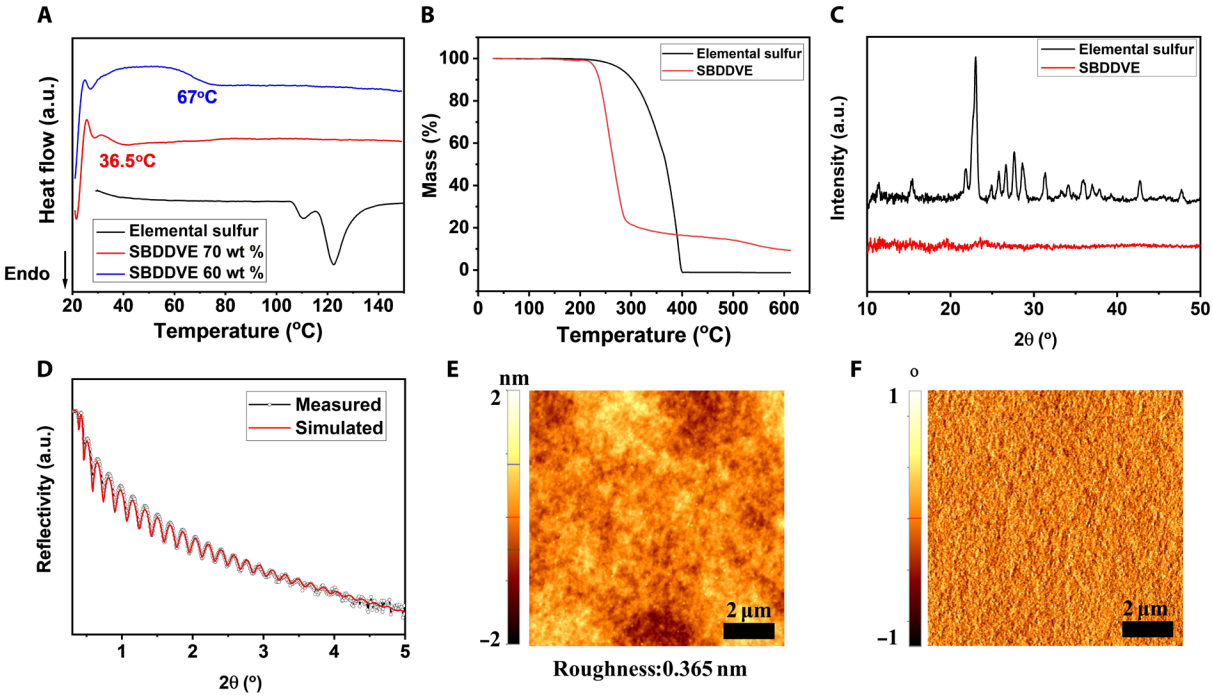

Fig. 2. Physical properties of sCVD polymers. Thermal and structural properties of the SBDDVE: (**A**) DSC spectra of 60 wt % SBDDVE (blue), 70 wt % SBDDVE (red), and elemental sulfur (black). a.u., arbitrary units. (**B**) TGA spectra of elemental sulfur (black) and 60 wt % SBDDVE (red). (**C**) X-ray diffraction (XRD) spectra of elemental sulfur (black) and 60 wt % SBDDVE (red). (**D**) XRR spectra of 60 wt % SBDDVE film (red) and the corresponding curve fit (black). (**E**) Atomic force microscopy (AFM) image of the 60 wt % SBDDVE film along with (**F**) AFM phase image.

amount of residual fraction was observed with SBDDVE, similar to the SCPs prepared from molten sulfur (Fig. 2B) (*18*). The DSC and TGA results illustrate that the SBDDVE was not a mere mixture of polymer with elemental sulfur but a tight SCP polymer network.

The x-ray diffraction (XRD) spectrum of the elemental sulfur shows typical sulfur-related crystalline peaks (Fig. 2C) (*19*), whereas no apparent crystallinity is detected from 100-nm-thick SBDDVE film in XRD spectrum regardless of the sulfur content, indicating that the SCPs are fully amorphous without unreacted residual sulfur (see fig. S3, A to E). From the x-ray reflectivity (XRR) analysis, the estimated density of the 50-nm-thick SBDDVE film was 1.58 g/cm^3 (Fig. 2D), which is between those of elemental sulfur (~2 g/cm^3) and BDDVE (0.898 g/cm^3), and the curve fit provides a good match with theoretical model for homogeneous film composition, indicating that the SCP composition is homogeneous, which is an advantageous characteristic of the vapor-phase method (see Supplementary Materials for more information about XRR). Atomic force microscopy (AFM) also displays that the surface of SBDDVE film is extremely smooth with the root mean square roughness of 0.365 nm without any noticeable phase separation or recrystallization of elemental sulfur (Fig. 2E). The AFM phase image indicated that the surface of the polymer was homogeneous without any apparent phase separation (Fig. 2F).

Fourier transform IR (FTIR) spectrum of SBDDVE showed S—S and C—S stretching at around 480 and 1080 cm^{-1}, respectively (Fig. 3B) (*17*, *20*, *21*). The spectrum also showed the peaks at 1100 and 2900 cm^{-1}, corresponding to the C—O—C and C—H stretching, respectively, from BDDVE monomer (*22*, *23*). The peak near 1600 cm^{-1}, representing the C═C stretching in BDDVE, was totally disappeared in the FTIR spectrum of SBDDVE, indicating that radical addition polymerization was performed fully between sulfur and divinyl comonomer (*24*). Considering the extremely low reactivity of vinyl ethers toward radical homopolymerization (*25*, *26*), SBDDVE thin films presumably contain alternating polysulfide-vinyl ether structure. Copolymerization of sulfur with various other vinyl ethers, allyl, and silane compounds was also confirmed by FTIR spectroscopy (see fig. S3, F and G). FTIR spectra of all comonomers used in this study showed C═C stretching band at 1600 cm^{-1} (*24*), which disappeared after the polymerization reaction. All FTIR spectra of SCPs showed characteristic sulfur-related peaks including the peaks corresponding to S—S and C—S stretching at around 480 and 1080 cm^{-1}, respectively, in accordance with the reaction between sulfur chain and vinyl functional groups in the corresponding monomer. No sulfur-related peaks are detected in the FTIR spectra of the corresponding polymers without sulfur incorporation. The SCPs from comonomers having ether moieties, SBDDVE and poly(sulfur-*co*-di(ethylene glycol)divinyl ether) (SDEGDVE), showed characteristic ether peaks at 1100 and 2900 cm^{-1}, corresponding to the C—O—C and C—H stretching peaks, respectively (*22*, *23*). The SCPs from allyl compounds, poly(sulfur-*co*-1,11-dodecadiene) (SDDDE) and poly(sulfur-*co*-1,9-decadiene) (SDDE), also showed characteristic peaks around 2900 cm^{-1}, representing the C—H stretching. Analogously in the FTIR spectra of polymers with organosilicon-containing monomers including 1,3,5-trivinyl-1,3,5-trimethylcyclotrisiloxane (V3D3), 1,3,5,7-tetravinyl-1,3,5,7-tetramethylcyclotetrasiloxane (V4D4), and hexavinyldisiloxane (HVDS), the peak at 1260 cm^{-1} corresponding to the Si—C bond is observed (*27*, *28*), confirming the full retention of the characteristic functional groups of each monomer, regardless of the monomer species. All the SCPs prepared by sCVD had not been reported to date by other synthesis method to date, which strongly suggest that a wide variety of SCPs can further be generated directly from elemental sulfur through sCVD in expanded manner,

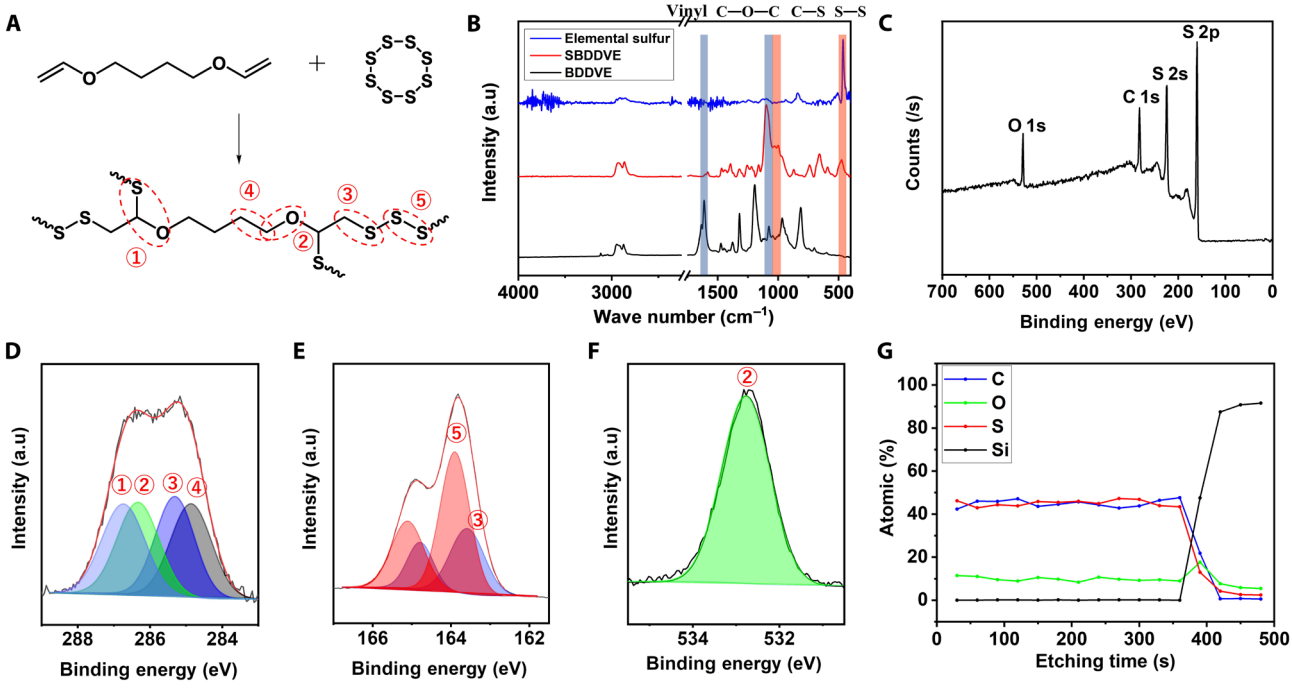

Fig. 3. Chemical analysis of sCVD SCP films. (**A**) A synthetic scheme of SBDDVE polymerization via sCVD using elemental sulfur. Chemical composition analysis of SBDDVE: (**B**) FTIR spectra of the elemental sulfur (top), SBDDVE (middle), and BDDVE monomer (bottom). Ether (C—O—C, 1100 cm^{-1}) and vinyl (C═C, 1600 cm^{-1}) peaks found in the monomer moiety are highlighted in blue, and sulfur (S—S, 480 cm^{-1}; C—S, 1080 cm^{-1}) peaks found in the sulfur moiety is highlighted in red. (**C**) XPS survey scan spectrum of SBDDVE-coated Si wafer and the corresponding (**D**) XPS C 1s high-resolution scan and its deconvoluted peaks featured with light blue for S—C—O, green for C—O, blue for C—S, and gray for C—C, respectively. (**E**) XPS S 2p high-resolution scans and its deconvoluted peaks in red for S—S and in blue for C—S. (**F**) XPS O 1s high-resolution scans and its deconvoluted peak in green for C—O. (**G**) XPS depth profile analysis of 300-nm-thick SBDDVE film coated on Si wafer.

regardless of their compatibility with sulfur in solid or liquid state. The results also demonstrate that this unique sulfur copolymerization method is a versatile platform for the preparation of high-sulfur content polymer thin films with tailored molecular structure and functions.

XPS was conducted to gather further information about the bond connectivity within the polymer matrix obtained from sCVD. The XPS survey spectrum showed characteristic SBDDVE peaks of S 2p, C 1s, and O 1s (Fig. 3C). The calculated surface C/O atomic ratio in SBDDVE was 78.9:21.1, consistent with the C/O ratio from the molecular structure of BDDVE (80:20). The estimated surface sulfur content in SBDDVE was 71.9 wt %, corresponding to 52.8 atomic %, which is a high value. High-resolution XPS analysis for each element was also performed (Fig. 3D), where the C 1s was deconvoluted to S—C—O, C—O, C—S, and C—C at 286.8, 286.3, 285.3, and 284.8 eV, respectively (*29*, *30*). The quantitative ratio among those peaks was 1:1.01:0.98:0.99, indicating that almost four C—S bonds were formed per BDDVE monomer, consistent with the expected alternating polysulfide-vinyl ether structure (Fig. 3A). Deconvolution of the S 2p peak into two doublets, representing C—S and S—S bonds at 164.8/163.6 eV and 165.1/163.9 eV, respectively (Fig. 3E) (*17*, *30*, *31*), gave an estimated C—S–to–S—S ratio of 1:1.96, from which the average polysulfide chain length (rank) was determined to be 5.92. Assuming that each C═C bond of BDDVE formed two C—S bonds, the calculated polysulfide rank was 5.67, which is quite similar with the estimation from the survey scan XPS data shown above. This suggests that each BDDVE unit is connected to nearly four polysulfide chains, indicating high degree of cross-linking. In addition, the O 1s spectrum showed only a single peak corresponding to BDDVE, indicating that no sulfur oxide formation arose during sCVD (Fig. 3F).

Depth profile XPS analysis results (Fig. 3G) showed that the composition of the SBDDVE film was consistent throughout the bulk of the film, confirming that the surface composition was identical to the internal composition. The analyses of SBDDVE obtained from sCVD indicate the formation of homogenous SCP film with high sulfur content and excellent smoothness in which sulfur is present as short, fragmented polysulfide chains, an ideal SCP structure for the prevention of depolymerization via S_8 elimination (*9*).

Optical properties of SCPs via sCVD

With the compositional information of SCPs through sCVD at hand, optical properties of the films were evaluated. Optically transparent polymers with high refractive index (n) and low extinction coefficient (k) had long been sought for various optical applications such as microlenses, optical waveguides, and photonic crystals (*3*). Despite extensive research efforts, it is still extremely difficult to find organic polymers with full transparency in the visible light region and $n > 1.7$.

Refractive index of a material is described through the Lorentz-Lorenz equation

$$n = \sqrt{\frac{1 + 2(R_M/V_M)}{1 - (R_M/V_M)}} \quad (1)$$

where the molar refraction (R_M) is the total atomic and functional group refraction (polarizability) of the material's constituents and molar volume (V_M) is the sum of the volume of a mole of constituent atom and functional groups divided by their respective formula weights. The relationship indicates that the moieties having high

molar refraction and low molar volume, such as sulfur, selenium, sulfones, and halogens, increase the refractive index of polymeric materials. Because of its ability to form a linear chain, sulfur is the most widely used moiety in an HRIPs. While polymers having majority sulfur content by weight has been demonstrated to n often exceeding 1.7, these polymers show large extinction coefficients in the visible range. A recently reported sulfur-rich polymers from inverse vulcanization, for example, while having $n > 1.8$, show strong absorption up to approximately 450 nm, rendering the material deep red (table S1).

To compare the optical properties of SBDDVE prepared through sCVD with poly(sulfur-*co*-1,3-diisopropenyl benzene) (SDIB) prepared from inverse vulcanization, we compared the optical properties of the thin films of the two polymers. While a 1.0-μm-thick SDIB thin film with 70 wt % sulfur contents demonstrated strong absorption in the blue region of the visible range, SBDDVE films, having thickness ranging from 100 nm to 1.8 μm, showed extremely high transparency throughout the entire visible range (Fig. 4A). The ultraviolet-visible (UV-vis) absorbance spectra of the SBDDVE films obtained from sCVD showed identical optical band edge over the film thickness range of 100 nm to 1.8 μm, indicating that the optical properties did not vary with thickness (see fig. S4, A and B). Considering the tendency of bathochromic shift in the UV-vis absorption of polysulfides with increasing rank (*32*), the extraordinary transparency in SBDDVE films from sCVD suggests excellent uniformity in the rank distribution of polysulfide chains within SBDDVE compared to those in SCPs obtained from molten sulfur (*33*). The narrow distribution of polysulfide rank and the subsequent absence of long polysulfide chains absorbing in the visible range are attributed to the speciation of sulfur vapor (*34*), which consists of molecules ranging from S_2 to S_8. In contrast, molten sulfur contains much longer linear sulfur chains (*33*) from equilibrium polymerization of sulfur, especially at the

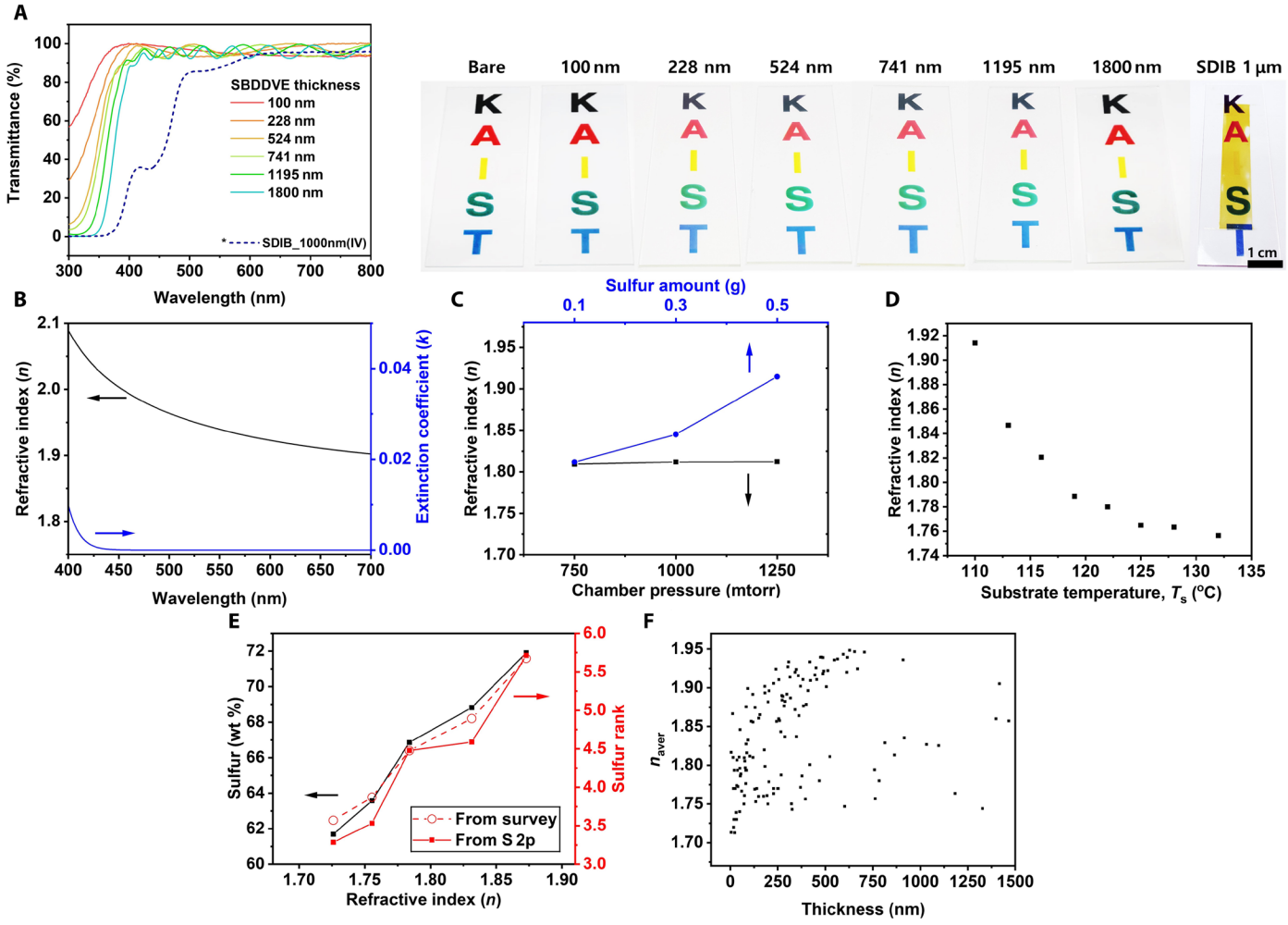

Fig. 4. Optical properties of the sCVD films. (**A**) Transmittance spectra of SBDDVE from sCVD with thickness ranging from 100 nm to 1.8 μm and SDIB from inverse vulcanization with a thickness of 1.0 μm with digital photographs of corresponding films coated on glass slides. (**B**) Refractive index (n) and extinction coefficient (k) of 500-nm-thick SBDDVE obtained using spectroscopic ellipsometry. (**C**) The sulfur loading amount (blue; with the fixed process pressure of 1000 mtorr and $T_s = 110$°C), the chamber pressure (black; with the fixed sulfur amount of 0.1 g and $T_s = 110$°C), and (**D**) the substrate temperature (with the fixed sulfur loading amount of 0.5 g and the process pressure of 1000 mtorr). (**E**) The sulfur weight ratio in SBDDVE calculated from XPS survey scan (black), sulfur rank calculated from XPS survey scan (red dash), and sulfur rank calculated from XPS S 2p high-resolution scan (red solid) with respect to the corresponding refractive index. (**F**) The average refractive index from 400 to 700 nm versus thickness plot of SBDDVE synthesized by sCVD. Photo credit: Wontae Jang (Korea Advanced Institute of Science and Technology) and Jisung Choi (Kyung Hee University).

temperature ranges at which copolymerization of molten sulfur is conducted.

Spectroscopic ellipsometry was also performed to analyze the optical properties of the SBDDVE formed via sCVD (Fig. 4B) and various other SCPs (see fig. S4, C to F). SBDDVE film showed a refractive index as high as 1.91 at 632.8 nm, which, to the best of our knowledge, is one of the highest values reported to date among organic polymers or polysulfide-containing polymers (*3*). The combination of excellent transparency and the ultrahigh *n*, attributed to the exceedingly high sulfur content with uniform distribution of polysulfide rank and high degrees of cross-linking, render SBDDVE from sCVD unique among HRIPs.

Optical materials display varying degrees of optical dispersion, or chromatic aberration, originating from wavelength-dependent changes in the refractive index. Optical dispersion is quantified by Abbe's number (ν_D), which is given by

$$\nu_D = \frac{n_D - 1}{n_F - n_C} \quad (2)$$

where n_D, n_F, and n_C are the refractive indices at the wavelength of the sodium D (589.3 nm), hydrogen F (486.1 nm), and hydrogen C (656.3 nm) lines, respectively. Higher ν_D indicates lower refractive index variation by wavelength. Despite the existence of a general trade-off relationship between *n* and ν_D, the degree of trade-off depends on the molar dispersion of constituent atoms and functional groups in a material. The ν_D values of polymers from sCVD are shown in table S2. While SBDDVE with $n = 1.915$ showed ν_D of 14.698, that of SBDDVE with $n = 1.726$ showed ν_D of 23.613, which is quite high values of SCPs with $n > 1.7$.

The effect of the sCVD process parameters on the properties of SCPs

The sCVD process parameters, including the substrate temperature (T_s), process pressure, and the amount of sulfur loading were controlled systematically to tailor the optical property of the sCVD polymer films. Before the sCVD, the process chamber was filled solely with the vaporized monomer to reach the target pressure; hence, the process pressure in sCVD corresponds to the measure of the input amount of the monomer. First of all, the effect of sulfur loading amount was monitored with the fixed process pressure, T_s, and process time to 1000 mtorr, 110°C, and 5 min, respectively (Fig. 4C). Increasing the loading amount of sulfur resulted in a distinct linear increase in the refractive index of SBDDVE. On the other hand, changing the amount monomer while keeping all the other parameters identical with 0.1 g of sulfur loading did not cause any noticeable tendency in refractive index variation (Fig. 4C). This observation indicates that sulfur is the rate-determining species in the vapor-phase polymerization as far as the monomer is sufficiently provided into the chamber. Increasing the T_s also induced a substantial decrease in the refractive index (Fig. 4D), along with decrease in film thickness (fig. S5). The observation is attributed to decreasing adsorption of sulfur and monomers to the substrate with increasing T_s (*35*–*37*). Furthermore, higher T_s would lead to increase in S—S bond dissociation, leading to a greater density of sulfur radicals within the deposited film. With the formation of C—S bonds being thermodynamically favorable, increased density of sulfur radicals would lead to a higher proportion of BDDVE being incorporated into the polymer matrix, decreasing the sulfur content and, hence, refractive index of the deposited film. The refractive index of the SBDDVE film is closely related with the sulfur content and, thus, the sulfur rank in the SCP film. The SCPs with higher refractive index, obtained by increasing the input sulfur amount and decreasing T_s, contain higher sulfur contents, estimated by the XPS survey scan. Because BDDVE does not readily homopolymerize through radical polymerization, increasing the sulfur content is accompanied by the increase in the length of polysulfide segments within the SCP network and, thus, leading to the increased refractive index. The sulfur rank could be calculated both from the XPS survey scan and high-resolution S 2p XPS scan results (see fig. S6 and table S4), as illustrated in the XPS analysis above (Fig. 2, C to E), showing similar tendency with each other; the sulfur rank, regardless of the estimation method, is commonly increased in accordance with the increasing sulfur content in SCPs and thus induced the increased refractive index (Fig. 4E).

Similarly, the thickness could also be controlled by tuning the deposition process parameters (see fig. S5). Increasing the sulfur amount and monomer input rate generated thicker film, while increasing the T_s decreases the thickness due to the limited adsorption of reactants. Systematic tuning of the process parameters of sCVD enabled us to build a series of SCP films with the wide range of refractive index and thickness (Fig. 4F), which is one of the most important features of sCVD process for the generation of various kinds of SCP films with designed refractive index and thickness and essentially important for the device applications requiring precise control of the optical property.

The sCVD process is performed in vapor phase to generate a highly cross-linked polymer network with uniform polymer composition. Especially, the heavily cross-linked monomer-sulfur network with shortly segmented polysulfide chain is advantageous to stabilize the SCP structure against various environmental and chemical stresses. It is well known that SCPs with high content of sulfur synthesized via other polymerization methods had suffered severely from the depolymerization and, thus, releasing elemental S_8 out from the SCP. For example, inverse vulcanization product from elemental sulfur and SDIB showed a notable degradation in 12 months of storage in air ambient (Fig. 5A), largely due to the depolymerization. On the other hand, the SBDDVE film with tightly cross-linked network showed no apparent degradation in its film morphology or loss in sulfur even after 2 years of storage in air ambient, presumably due to the narrow distribution of the short polysulfide chain length in SCP (Fig. 5A). The sCVD SBDDVE film also showed an excellent stability against various kinds of common organic solvents including water, acetone, toluene, and *n*-hexane; no variation in thickness or refractive index was detected in 2 hours of incubation in each solvent (Fig. 5, B and C). The outstanding environmental stability of the SCPs via sCVD is highly desirable for long-term, stable utilization of the materials.

DISCUSSION

A previously unknown one-step dry deposition method, sCVD, was devised for preparing polymer thin films with high sulfur content directly from elemental sulfur. The method allows for the formation of highly cross-linked SCP thin films, the properties of which could be tuned exquisitely by varying the polymerization parameters. The vapor phase process allows for the use of various kinds of comonomers regardless of the miscibility with elemental sulfur in the liquid phase, which extends the scope of SCPs from elemental sulfur. FTIR

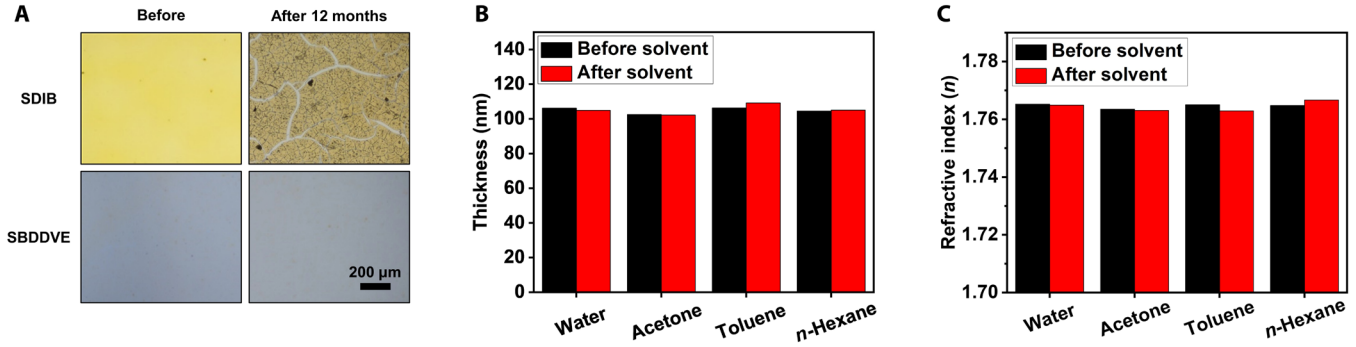

Fig. 5. Environmental stability of the sCVD films. (**A**) Optical microscopy images of glass coated with SDIB synthesized by inverse vulcanization before (left) and after (right) storage under ambient air for 12 months and SBDDVE film synthesized by sCVD before and after the storage under ambient air for 24 months. (**B**) Thickness and (**C**) refractive index of silicon wafer coated with 100-nm-thick SBDDVE polymer film before (black) and after (red) solvent test with water, acetone, toluene, and *n*-hexane for 2 hours.

and XPS analyses showed that the polymerization occurred readily without the formation of elemental sulfur, unreacted monomers, and phase-separated domains, giving extremely smooth thin films with excellent stability. These features clearly distinguish the SCPs from those synthesized in the liquid phase. The refractive index higher than 1.9 could be achieved, which is the highest refractive index value obtained from an organic material to date. Moreover, the SCP film showed outstanding optical transparency in entire visible light region, presumably due to the uniformly dispersed, short-segment polysulfide chains, which is a distinct feature unachievable in polymerizations with molten sulfur. The versatile process does not require any additional solvent, additive, nor catalyst. Moreover, the high-performance polymer film can be created in simple one-step manner, which is highly advantageous considering the extremely complicated synthesis methods currently used for the synthesis of SCPs with high refractive index. The colorless organic film with unprecedentedly high refractive index will serve as platform materials for future high-end optical device applications.

MATERIALS AND METHODS

Synthesis of SCP

SBDDVE, SDEGDVE, SDDDE, SDDE, poly(sulfur-*co*-1,3,5-trivinyl-1,3,5-trimethylcyclotrisiloxane), poly(sulfur-*co*-1,3,5,7-tetravinyl-1,3,5,7-tetramethylcyclotetrasiloxane), and poly(sulfur-*co*-hexavinyldisiloxane) were prepared using a custom-built sCVD reactor on various substrates including slide glass, Si wafer, stainless steel mesh, PET, PEN, PI, PDMS, and latex glove. Elemental sulfur (99%; Sigma-Aldrich) was loaded in source cell located at the bottom in the sCVD reactor and was heated to 180°C to evaporate elemental sulfur. The monomer, BDDVE (98%; Sigma-Aldrich), DEGDVE (99%; Sigma-Aldrich), 1,11-dodecadiene [DDDE; 99%; Tokyo Chemical Industry (TCI)], 1,9-decadiene (DDE; 98%; TCI), V3D3 (95%; Gelest), V4D4 (95%; Gelest), and HVDS (95%; Gelest) were vaporized and introduced into the sCVD reactor simultaneously with sulfur evaporation. All the chemicals in this work were used as purchased without further purification. To obtain the required chamber pressure, BDDVE and DEGDVE were heated to 60°C; DDDE was heated to 70°C; V3D3, V4D4, and HVDS were heated to 80°C; and DDE was maintained at room temperature. To control the thickness and refractive index of sulfur copolymer films, temperature of substrate, amount of sulfur loading, and chamber pressure were controlled systematically. In all cases, the filament temperature was kept at 350°C, and the chamber wall was heated to 75°C to minimize the adsorption of unnecessary chemicals.

Characterization of the synthesized SCPs films

Cross-sectional images were obtained using scanning electron microscope [Nova 230, Field Electron and Ion Company (FEIC)]. TGA and DSC were performed in the range from 25° to 600°C (heating rate was maintained with 10°C/min) using LABSYS evo TGA-DSC instrument. The crystallinity was measured by x-ray diffractometer (Rigaku D/MAX-RC, 12 kW) with a scanning range from 10° to 70°. The x-ray reflectivity (XRR) spectra were obtained using a Rigaku SmartLab x-ray diffractometer using x-rays with a wavelength (λ) of 1.541 Å. AFM images were taken by a scanning probe microscope (XE-100, Park Systems) at a scan size of 10 μm by 10 μm. FTIR spectra were obtained using ALPHA FTIR in absorbance mode (Bruker Optics). A total of 64 scans were collected and averaged for each spectrum. The XPS and high-resolution spectra results were obtained using Sigma Probe Multipurpose XPS (Thermo VG Scientific) with a monochoromatized Al Kα source.

Optical property analysis

The optical transmittance of the SCP film was measured using a UV-vis spectrometer (UV-3600, Shimadzu, Kyoto, Japan) with air base using a bare glass slide as a reference within the wavelengths of the visible spectrum (150 to 1000 nm). The refractive index and thickness were obtained by a spectroscopic ellipsometer (M2000, J. A. Woollam, USA). To check the uniformity of sCVD system, the upper, middle, and lower portions of the sulfur copolymer films on the 10 mm by 75 mm wafer were measured respectively.

Stability test

Chemical stability of SBDDVE films was tested by measuring the thickness and refractive index of SBDDVE films before and after exposing the films to various organic solvents. SBDDVE films on wafer were soaked in deionized water, acetone (99.8%; Sigma-Aldrich), isopropyl alcohol (99.8%; Sigma-Aldrich), and *n*-hexane (95%; DaeJung). After 2 hours of soaking, the samples were rinsed thoroughly with deionized water and dried with N_2 gas for the measurement of refractive index and thickness.

SUPPLEMENTARY MATERIALS

Supplementary material for this article is available at http://advances.sciencemag.org/cgi/content/full/6/28/eabb5320/DC1

REFERENCES AND NOTES

1. J. J. Griebel, S. Namnabat, E. T. Kim, R. Himmelhuber, D. H. Moronta, W. J. Chung, A. G. Simmonds, K.-J. Kim, J. van der Laan, N. A. Nguyen, E. L. Dereniak, M. E. Mackay, K. Char, R. S. Glass, R. A. Norwood, J. Pyun, New infrared transmitting material via inverse vulcanization of elemental sulfur to prepare high refractive index polymers. *Adv. Mater.* **26**, 3014–3018 (2014).
2. L. E. Anderson, T. S. Kleine, Y. Zhang, D. D. Phan, S. Namnabat, E. A. LaVilla, K. M. Konopka, L. Ruiz Diaz, M. S. Manchester, J. Schwiegerling, R. S. Glass, M. E. Mackay, K. Char, R. A. Norwood, J. Pyun, Chalcogenide hybrid inorganic/organic polymers: Ultrahigh refractive index polymers for infrared imaging. *ACS Macro Lett.* **6**, 500–504 (2017).
3. T. Higashihara, M. Ueda, Recent progress in high refractive index polymers. *Macromolecules* **48**, 1915–1929 (2015).
4. Y. Suzuki, T. Higashihara, S. Ando, M. Ueda, Synthesis of high refractive index poly (thioether sulfone) s with high Abbe's number derived from 2,5-is (sulfanylmethyl)-l,4-dithiane. *Polymer J.* **41**, 860–865 (2009).
5. Y. Suzuki, T. Higashihara, S. Ando, M. Ueda, Synthesis and characterization of high refractive index and high Abbe's number poly(thioether sulfone)s based on tricyclo [5.2.1.$0^{2,6}$] decane moiety. *Macromolecules* **45**, 3402–3408 (2012).
6. T. S. Kleine, N. A. Nguyen, L. E. Anderson, S. Namnabat, E. A. LaVilla, S. A. Showghi, P. T. Dirlam, C. B. Arrington, M. S. Manchester, J. Schwiegerling, R. S. Glass, K. Char, R. A. Norwood, M. E. Mackay, J. Pyun, High refractive index copolymers with improved thermomechanical properties via the inverse vulcanization of sulfur and 1,3,5-triisopropenylbenzene. *ACS Macro Lett.* **5**, 1152–1156 (2016).
7. J. J. Griebel, N. A. Nguyen, S. Namnabat, L. E. Anderson, R. S. Glass, R. A. Norwood, M. E. Mackay, K. Char, J. Pyun, Dynamic covalent polymers via inverse vulcanization of elemental sulfur for healable infrared optical materials. *ACS Macro Lett.* **4**, 862–866 (2015).
8. W. J. Chung, J. J. Griebel, E. T. Kim, H. Yoon, A. G. Simmonds, H. J. Ji, P. T. Dirlam, R. S. Glass, J. J. Wie, N. A. Nguyen, B. W. Guralnick, J. Park, A. Somogyi, P. Theato, M. E. Mackay, Y.-E. Sung, K. Char, J. Pyun, The use of elemental sulfur as an alternative feedstock for polymeric materials. *Nat. Chem.* **5**, 518–524 (2013).
9. J. J. Griebel, R. S. Glass, K. Char, J. Pyun, Polymerizations with elemental sulfur: A novel route to high sulfur content polymers for sustainability, energy and defense. *Prog. Polym. Sci.* **58**, 90–125 (2016).
10. A. V. Tobolsky, A. Eisenberg, Equilibrium polymerization of sulfur. *J. Am. Chem. Soc.* **81**, 780–782 (1959).
11. A. V. Tobolsky, Polymeric sulfur and related polymers. *J. Polymer Sci.* **12**, 71–78 (1966).
12. T. S. Kleine, R. S. Glass, D. L. Lichtenberger, M. E. Mackay, K. Char, R. A. Norwood, J. Pyun, 100th anniversary of macromolecular science viewpoint: High refractive index polymers from elemental sulfur for infrared thermal imaging and optics. *ACS Macro Lett.* **9**, 245–259 (2020).
13. T. S. Kleine, T. Lee, K. J. Carothers, M. O. Hamilton, L. E. Anderson, L. Ruiz Diaz, N. P. Lyons, K. R. Coasey, W. O. Parker Jr., L. Borghi, M. E. Mackay, K. Char, R. S. Glass, D. L. Lichtenberger, R. A. Norwood, J. Pyun, Infrared fingerprint engineering: A molecular-design approach to long-wave infrared transparency with polymeric materials. *Angew. Chem. Int. Ed.* **58**, 17656–17660 (2019).
14. A. M. Coclite, P. Lund, R. Di Mundo, F. Palumbo, Novel hybrid fluoro-carboxylated copolymers deposited by initiated chemical vapor deposition as protonic membranes. *Polymer* **54**, 24–30 (2013).
15. M. J. Kwak, M. S. Oh, Y. Yoo, J. B. You, J. Kim, S. J. Yu, S. G. Im, Series of liquid separation system made of homogeneous copolymer films with controlled surface wettability. *Chem. Mater.* **27**, 3441–3449 (2015).
16. X. Wu, J. A. Smith, S. Petcher, B. Zhang, D. J. Parker, J. M. Griffin, T. Hasell, Catalytic inverse vulcanization. *Nat. Commun.* **10**, 647 (2019).
17. I. Gomez, D. Mecerreyes, J. A. Blazquez, O. Leonet, H. Ben Youcef, C. Li, J. L. Gómez-Cámer, O. Bondarchuk, L. Rodriguez-Martine, Inverse vulcanization of sulfur with divinylbenzene: Stable and easy processable cathode material for lithium-sulfur batteries. *J. Power Sources* **329**, 72–78 (2016).
18. D. J. Parker, H. A. Jones, S. Petcher, L. Cervini, J. M. Griffin, R. Akhtar, T. Hasell, Low cost and renewable sulfur-polymers by inverse vulcanisation, and their potential for mercury capture. *J. Mater. Chem. A* **5**, 11682–11692 (2017).
19. Y. Zhao, F. Yin, Y. Zhang, C. Zhang, A. Mentbayeva, N. Umirov, H. Xie, Z. Bakenov, A free-standing sulfur/nitrogen-doped carbon nanotube electrode for high-performance lithium/sulfur batteries. *Nanoscale Res. Lett.* **10**, 450 (2015).
20. Z. Sun, M. Xiao, S. Wang, D. Han, S. Song, G. Chen, Y. Meng, Sulfur-rich polymeric materials with semi-interpenetrating network structure as a novel lithium–sulfur cathode. *J. Mater. Chem. A* **2**, 9280–9286 (2014).
21. H. Ding, J.-S. Wei, H.-M. Xiong, Nitrogen and sulfur co-doped carbon dots with strong blue luminescence. *Nanoscale* **6**, 13817–13823 (2014).
22. B. C. Smith, The CO bond III: Ethers by a knockout. *Spectroscopy* **32**, 22–26 (2017).
23. W. S. O'Shaughnessy, M. Gao, K. K. Gleason, Initiated chemical vapor deposition of trivinyltrimethylcyclotrisiloxane for biomaterial coatings. *Langmuir* **22**, 7021–7026 (2006).
24. H. Moon, H. Seong, W. C. Shin, W.-T. Park, M. Kim, S. Lee, J. H. Bong, Y.-Y. Noh, B. J. Cho, S. Yoo, S. G. Im, Synthesis of ultrathin polymer insulating layers by initiated chemical vapour deposition for low-power soft electronics. *Nat. Mater.* **14**, 628–635 (2015).
25. D. Braun, F. Hu, Polymers from non-homopolymerizable monomers by free radical processes. *Prog. Polym. Sci.* **31**, 239–276 (2006).
26. J. Choi, J. Yoon, M. J. Kim, K. Pak, C. Lee, H. Lee, K. Jeong, K. Ihm, S. Yoo, B. J. Cho, H. Lee, S. G. Im, Spontaneous generation of a molecular thin hydrophobic skin layer on a sub-20 nm, high-*k* polymer dielectric for extremely stable organic thin-film transistor operation. *ACS Appl. Mater. Interfaces* **11**, 29113–29123 (2019).
27. G. Aresta, J. Palmans, M. C. van de Sanden, M. Creatore, Initiated-chemical vapor deposition of organosilicon layers: Monomer adsorption, bulk growth, and process window definition. *J. Vac. Sci. Technol. A* **30**, 041503 (2012).
28. M. B. Sassin, J. W. Long, J. M. Wallace, D. R. Rolison, Routes to 3D conformal solid-state dielectric polymers: Electrodeposition *versus* initiated chemical vapor deposition. *Mater. Horiz.* **2**, 502–508 (2015).
29. A. Abdul Razzaq, Y. Yao, R. Shah, P. Qi, L. Miao, M. Chen, X. Zhao, Y. Peng, Z. Deng, High-performance lithium sulfur batteries enabled by a synergy between sulfur and carbon nanotubes. *Energy Storage Mater.* **16**, 194–202 (2019).
30. J. Ye, F. He, J. Nie, Y. Cao, H. Yang, X. Ai, Sulfur/carbon nanocomposite-filled polyacrylonitrile nanofibers as a long life and high capacity cathode for lithium–sulfur batteries. *J. Mater. Chem. A* **3**, 7406–7412 (2015).
31. H. Kim, J. Lee, H. Ahn, O. Kim, M. J. Park, Synthesis of three-dimensionally interconnected sulfur-rich polymers for cathode materials of high-rate lithium–sulfur batteries. *Nat. Commun.* **6**, 7278 (2015).
32. B. Meyer, K. Spitzer, Extended Hückel calculations on the color of sulfur chains and rings. *J. Phys. Chem.* **76**, 2274–2279 (1972).
33. B. Meyer, Elemental sulfur. *Chem. Rev.* **76**, 367–388 (1976).
34. R. Steudel, Y. Steudel, M. W. Wong, Speciation and thermodynamics of sulfur vapor, in *Elemental Sulfur and Sulfur-Rich Compounds I* (Springer, 2003), pp. 117–134.
35. S. J. Yoon, K. Pak, T. Nam, A. Yoon, H. Kim, S. G. Im, B. J. Cho, Surface-localized sealing of porous ultralow-*k* dielectric films with ultrathin (< 2 nm) polymer coating. *ACS Nano* **11**, 7841–7847 (2017).
36. Y. I. Lee, N. J. Jeon, B. J. Kim, H. Shim, T.-Y. Yang, S. I. Seok, J. Seo, S. G. Im, A low-temperature thin-film encapsulation for enhanced stability of a highly efficient perovskite solar cell. *Adv. Energy Mater.* **8**, 1701928 (2018).
37. S. J. Yu, K. Pak, M. J. Kwak, M. Joo, B. J. Kim, M. S. Oh, J. Baek, H. Park, G. Choi, D. H. Kim, J. Choi, Y. Choi, J. Shin, H. Moon, E. Lee, S. G. Im, Initiated chemical vapor deposition: A versatile tool for various device applications. *Adv. Eng. Mater.* **20**, 1700622 (2018).
38. M. Yasaka, X-ray thin-film measurement techniques V. X-ray reflectivity measurement. *Rigaku J.* **26**, 1–9 (2010).
39. H. Kim, B.-C. Ku, M. Goh, H. C. Ko, S. Ando, N.-H. You, Synergistic effect of sulfur and chalcogen atoms on the enhanced refractive indices of polyimides in the visible and near-infrared regions. *Macromolecules* **52**, 827–834 (2019).

Acknowledgments

Funding: This work was supported by the Wearable Platform Materials Technology Center (WMC) funded by the National Research Foundation of Korea (NRF) Grant by the Korean Government (MSIT; no. 2016R1A5A1009926), by NRF grants funded by the Korean Government (MSIT; no. 2017R1A2B3007806), and by the Center for Advanced Soft-Electronics, which is funded by the Ministry of Science, ICT, and Future Planning, through the Global Frontier Project (CASE-2017M3A6A5052509). **Author contributions:** D.H.K., W.J., K. Choi, and S.G.I. conceived and designed the sCVD system. D.H.K., W.J., and K. Choi designed the experiments on the use of sCVD to fabricate SCPs and HRIP. D.H.K., W.J., J.S.C., and J.L. contributed on characterizing the chemistry of sCVD-based polymers and analysis of optical properties. D.H.K., W.J., J.P., J.L., K. Char, and S.G.I. prepared the manuscript. All authors discussed the results and contributed to the paper. All authors discussed the results and contributed to the paper. **Competing interests:** D.H.K., W.J., K. Choi, and S.G.I. are inventors on a patent application related to this work. Filed by Korea Advanced Institute of Science and Technology (KAIST) (10-2020-0021570, 2 February 2020). The authors declare that they have no other competing interests. **Data and materials availability:** All data needed to evaluate the conclusions in the paper are present in the paper and/or the Supplementary Materials. Additional data related to this paper may be requested from the authors.

Submitted 2 March 2020
Accepted 22 May 2020
Published 8 July 2020
10.1126/sciadv.abb5320

Citation: D. H. Kim, W. Jang, K. Choi, J. S. Choi, J. Pyun, J. Lim, K. Char, S. G. Im, One-step vapor-phase synthesis of transparent high refractive index sulfur-containing polymers. *Sci. Adv.* **6**, eabb5320 (2020).